Atmospheric Pollution Research

Chemical profiles of urban fugitive dust over Xi'an in the south margin of the Loess Plateau, China

Qian Zhang [1,2], **Zhenxing Shen** [1,2], **Junji Cao** [2], **KinFai Ho** [4], **Renjian Zhang** [3], **Zengjun Bie** [1], **Hairu Chang** [1], **Suixin Liu** [2]

[1] Department of Environmental Science and Engineering, Xi'an Jiaotong University, Xi'an 710049, China
[2] Key Laboratory of Aerosol, SKLLQG, Institute of Earth Environment, Chinese Academy of Sciences, Xi'an 710075, China
[3] Key Laboratory of Regional Climate-Environment Research for Temperate East Asia, Institute of Atmospheric Physics, Chinese Academy of Sciences, Beijing 100029, China
[4] Jockey Club School of Public Health and Primary Care, The Chinese University of Hong Kong, Shatin, Hong Kong, China

ABSTRACT

Urban fugitive dust samples were collected to determine the chemical profiles of fugitive dust over Xi'an. Seventy eight samples were collected and divided into categories of paved road dust, construction dust, cement dust, and soil dust. Eighteen elements, including Na, Mg, Al, Si, K, Ca, Ti, V, Cr, Mn, Fe, Co, Ni, Cu, Zn, As, Ba, and Pb, and eight water–soluble inorganic ions, including Na^+, Mg^{2+}, Ca^{2+}, NH_4^+, F^-, Cl^-, NO_3^- and SO_4^{2-}, were measured. The most abundant elements in these urban dust samples were Al, Si, Ca, and Fe. Al, Si, K, and Ti and showed strong positive correlations with each other, indicating they are typical dust trace elements. In contrast, elements of Ca, Zn, As, and Pb had negative correlations to crustal elements. Si/Al, K/Al, Ti/Al, Mn/Al, and Fe/Al ratios varied insignificantly among these four samples types; these ratios are similar to the properties of loess, desert, and Gobi soil dust reported in previous studies. A significantly higher Ca/Al ratio was dominant in the chemical profile of the cement samples. In addition, high Pb/Al and Zn/Al ratios were detected in comparison with those in the Gobi soil, desert soil, and loess soil samples, which indicated that Pb/Al and Zn/Al ratios can be considered as markers of urban dust. Total water–soluble ions occupied only a small fraction (<5%) in the urban fugitive soil samples indicating that most of the materials in the fugitive dust were insoluble. Ca^{2+} and SO_4^{2-} were the most abundant ions in all samples. Most of the Ca and K in the fugitive soil samples were in insoluble phases, which differ significantly in comparison with combustion sources. A strong correlation was observed between Ca^{2+} and estimated CO_3^{2-} levels indicating that most of Ca^{2+} was in the form of $CaCO_3$ rather than other calcium minerals in Xi'an fugitive dust.

Keywords: Urban fugitive dust, elements, water–soluble ions

Corresponding Author:
Zhenxing Shen
☎ : +86-29-82665227
🖷 : +86-29-82668789
✉ : zxshen@mail.xjtu.edu.cn

1. Introduction

High particulate matter (PM) level is a severe problem in most Chinese cities (Cao et al., 2005; Yang et al., 2011; Cao et al., 2012a). Except for contributions from fuel combustion and secondary aerosol formation, a substantial fraction of PM is contributed by fugitive dust, particularly in northern Chinese cities located in arid and semi arid regions. Fugitive dust sources include soil dust (Taylor and Mclennan, 1995; Zhang et al., 2002; Ashbaugh et al., 2003; Ta et al., 2003; Arimoto et al., 2006; Cao et al., 2008; Wu et al., 2011), paved and unpaved road dust (Vega et al., 2001; Ho et al., 2003a; Han et al., 2007; Bhaskar and Sharma, 2008; Amato et al., 2009; Cheng et al., 2011; Acosta et al., 2011), construction dust (Chow et al., 2003), and cement (Vega et al., 2001; Ho et al., 2003a; Abdul–Wahab, 2006; Cesari et al., 2012; Pietrodangelo et al., 2013). As mentioned by Cao et al. (2012a), geological materials have been shown to occupy 12%–34% of winter $PM_{2.5}$ mass and 17%–32% of summer $PM_{2.5}$ mass in 14 Chinese cities. Owing to the scarceness of chemical profiles of regional fugitive dust, previous studies have always used trace elements to estimate fugitive dust mass and to evaluate its sources. For example, elements of Si, Al, Fe, and Ca are considered as key markers and main components of fugitive dust to illustrate its contribution to urban aerosol particles (Ho et al., 2003b; Zhao et al., 2010; Cao et al., 2012a). Considering that elemental components vary with geographic locations and

background soil properties, such methods have over– or underestimated the fugitive dust mass when it was short of local chemical compositions. Moreover, because the chemical profiles vary with geography and the rapid changes in urban areas that occur during the years, it is necessary to analyze the characteristics of fugitive dust to establish the various source profiles.

Xi'an, the largest city in northwestern China, is located on the Guanzhong Plain at the southern edge of the Loess Plateau and has a residential population of 8 000 000 with 2 000 000 visitors per year. Because this city is located in the semi–arid region of China and precipitation is limited (approximately 600 mm per year), an imbalance occurs among the four seasons (Shen et al., 2012). Such conditions combine with the rapid increase in construction and heavy traffic to create severe fugitive dust pollution that threatens air quality in Xi'an (Zhang et al., 2002; Shen et al., 2011; Cao et al., 2012b). Although prior studies have focused on the chemical characteristics of PM in Xi'an (Cao et al., 2005; Shen et al., 2009a; Shen et al., 2011; Cao et al., 2012a), few mention the chemical profile of fugitive dust. In the present study, urban fugitive dust samples are obtained to develop fugitive dust chemical profiles. This research will contribute to studies that trace fugitive dust origin or that estimate its contribution to urban PM.

2. Methodology

2.1. Sample collection

Seventy eight urban fugitive dust samples were collected between March 30, 2012, and April 22, 2012 on and near the second ring road of Xi'an. On the basis of the sampling location, the following four types of dust samples were collected: (1) building construction dust, which was collected from building sites; (2) paved road dust, which was sampled from the city's main street; (3) fresh soil dust, which was collected during foundation excavation at construction sites; (4) cement samples collected in construction sites. 18, 46, 8, and 6, samples were obtained from the four sites, respectively. The sampling locations are shown in Figure 1. All samples were swept from the representative areas of the ground surface by using a plastic brush and tray. Sample collection was performed for nearly two weeks during early spring. The weather conditions were cloudy or sunny, and no precipitation occurred during the sampling period. Each sample (3–9 g) was placed into a sealing bag, then sieved through Tyler 200 mesh sieves, oven–dried at approximately 50 °C for 6 h, and kept in a Kraft bag under dry and cool conditions (Vega et al., 2001).

2.2. Chemical analysis

Each sieved sample (4–6 g) was weighed and pressed by using the sheeting method, which pressed the samples into circular pieces with 32 mm diameters under a force of 30 N for 20 sec. Element compositions were analyzed after being exposed to high–sensitivity X–ray fluorescence (XRF) at 30 °C for 22 min. Eighteen elements, including Na, Mg, Al, Si, K, Ca, Ti, V, Cr, Mn, Fe, Co, Ni, Cu, Zn, As, Pb, and Hg, were analyzed for each sample. The detection limits of XRF for chemical species were less than 0.01 $\mu g/m^3$. Detailed description of XRF analysis was given by Rhodes et al. (1972).

In preparation for analysis of cations and anions, including Na^+, NH_4^+, K^+, Mg^{2+}, Ca^{2+}, F^-, Cl^-, NO_3^-, and SO_4^{2-}), 10 mg samples were weighed and dissolved, then placed into separate 20 mL vials containing 10 mL distilled and deionized water with a resistivity of 18.3 MΩ. The vials were then placed in an ultrasonic water bath for 60 min and were shaken by a mechanical shaker for 1 hr for complete extraction of the ionic compounds. The extracts were filtered twice with a 0.45 μm pore size microporous membrane, and the filtrates were stored at 4 °C in a clean tube prior to analysis. The series of concentrations were analyzed by ion chromatography (IC, Dionex 500, Dionex Corp., Sunnyvale, California, United States). Cation (Na^+, NH_4^+, K^+, Mg^{2+}, and Ca^{2+}) concentrations were determined by using a CS12A column (Dionex Company) with 20 mM MSA eluent. Anions (F^-, Cl^-, NO_3^-, and SO_4^{2-}) were separated by an AS11–HC column (Dionex Company) by using 8 mM $NaCO_3$/1 mM $NaHCO_3$ as the eluent. The limits of detection were less than 0.05 mg/L for analysis. One sample in each group of ten was selected for a second analysis for quality control purposes. For quality assurance, the test standards followed the Standard Reference Center for Certified Reference Material produced by the National Research Center for Certified Reference Materials, China. A detail description of the ion analysis can be found in Shen et al. (2009a).

2.3. Enrichment factors

Enrichment factors (EFs) have been widely used in aerosol studies to differentiate the element origins between natural sources and anthropogenic emissions and to evaluate the degree of human activity influence. This process is a simple, semi–quantitative method of determining whether the elemental concentrations in the samples of interest are enriched or consistent with that expected from the amount of crustal/mineral matter in the sample. In this study, Al was used as a reference element, and the compositions of the Earth's upper continental crust (UCC) were taken from Taylor and Mclennan (1995). EFs were calculated by the following equation:

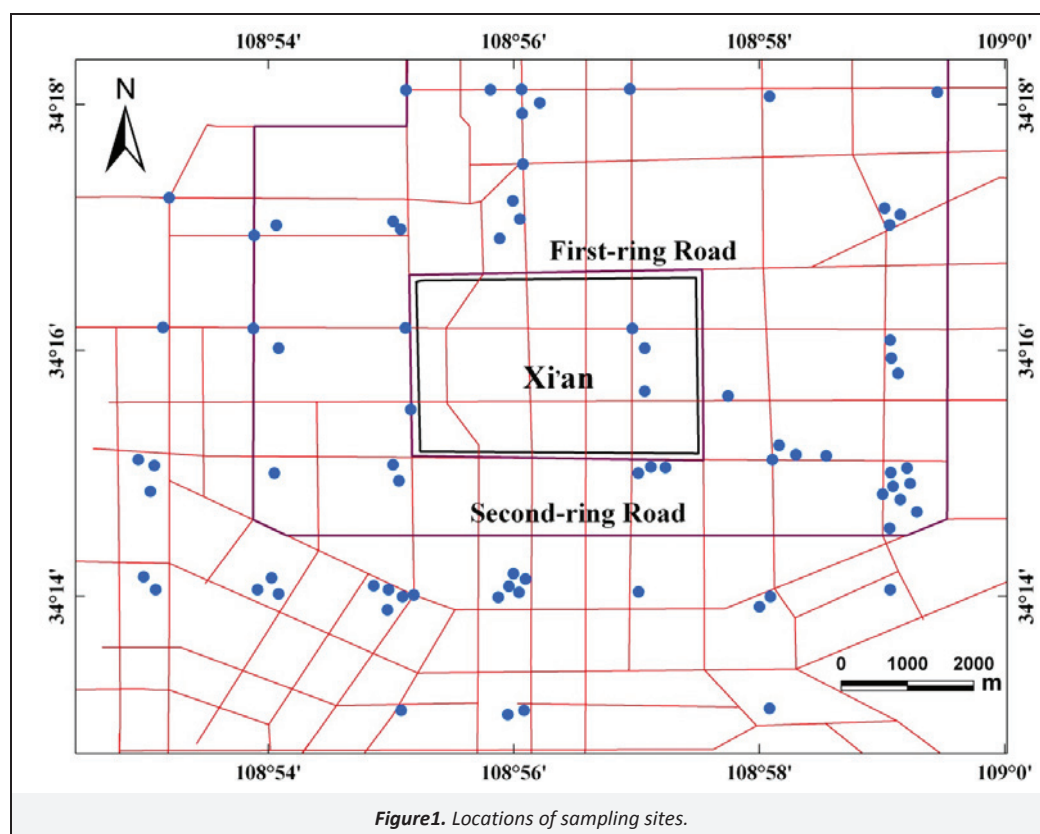$$EF_{crust}=(X/Al)_{samples}/(X/Al)_{crust} \tag{1}$$

Figure1. *Locations of sampling sites.*

X refers to the concentration of the specific element. The EF is often used in soil or aerosol samples to calculate the enriched elements of fugitive dust in Xi'an (Taylor and Mclennan, 1995; Shen et al., 2007; Cao et al., 2008) and was used as such here. Generally, if the EF of an element is higher than 5, that element has significant enrichment in comparison with Earth's UCC (Zhang et al., 2002; Zhang et al., 2005). Cesari et al. (2012) showed that this threshold is generally dependent on the reference composition used for the upper crust if local or the Earth's average otherwise. The two–threshold system is used to identify enriched elements for atmospheric PM_{10} and re–suspended PM_{10} (Cesari et al., 2012).

3. Results and Discussion

3.1. Elemental composition

Table 1 shows the chemical profiles of the four sample types. Generally, Si, Ca, Al, and Fe were the most abundant elements in all samples. Si concentration was the highest among the detected elements, followed by Ca, Al, and Fe in all except for the concrete samples, in which the Ca concentration was slightly higher than that of Si. It is clear that the elemental concentrations for construction and paved road samples are similar, which implies that such roads in the Xi'an area have similar sources. In contrast, cement samples showed a high Ca content that was nearly twice that exhibited by other sample types. Chow (1992a, 1992b) reported that the high Ca content in cement dust is similar to that in construction dust, whereas Yatkin and Bayram (2008) reported that Ca was present in larger proportions in the emissions of cement industry worldwide, which varied between 19% and 36%. Therefore, although it was slightly lower than that reported in the aforementioned studies, the highest abundance of Ca (17.3%) in this study may correlate to the characteristics of location and can also represent the specific characteristics of local cement production in this study (Table 1). The soil dust samples exhibited high Si but low Ca. It was also noted that Fe occupied 2.4% to 3.2% in all type samples, which was 4% lower than that of the Fe in mineral dust from desert or Gobi areas in northern China (Zhang et al., 2003). Therefore, the fugitive dust concentration was underestimated when Fe was used as a marker to estimate the mineral dust loading.

Elemental ratios can be considered as markers to trace the origin of soil dust in various desert regions (Alfaro et al., 2003; Arimoto, et al., 2004; Shen et al., 2007). In this study, the ratios of elements (Si, K, Ca, Ti, Mn, and Fe) to Al in fugitive dust samples were calculated and compared with dust samples from other regions (Table 2). In general, Si/Al, K/Al, Ti/Al, Mn/Al, and Fe/Al ratios varied insignificantly among these four sample types. However, the Ca/Al ratio in cement samples was the highest, followed by construction dust, paved road dust, and soil dust samples. Therefore, with the exception of the Ca/Al ratio, these relatively stable elemental ratios can represent the chemical profiles of fugitive dust in Xi'an when compared with other cities or for source apportionment applications based on chemical mass balance.

To further highlight the elemental composition of fugitive dust over Xi'an, the majority of elemental ratios in fugitive dust or desert soil dust reported in previous research are listed in Table 2. The Ca/Al ratios in soil dust in Chinese desert regions range from 0.74 to 1.9 (Arimoto et al., 2006; Shen et al., 2007; Cao et al., 2008), which were similar to urban dust samples in this study that, except for the cement samples, showed an abundance of Ca and a ratio Ca/Al higher or even twice that of the other types. High Ca concentrations in cement samples were also observed in Hong Kong and Mexico City (Vega et al., 2001; Ho et al., 2003a), in which the Ca/Al ratios were significantly higher. In contrast, the Ca/Al ratios in paved road dust in these two cities decreased substantially, which is similar to the values detected in Xi'an. Because the

cement samples were rich in Ca, one can assume that the cement dust came from the construction site if a high Ca level is detected in the fugitive dust. A study in California showed similar Ca/Al values between paved road dust and construction dust (Chow et al., 2003); however, the values were both lower than those measured in the present study. Kong et al. (2011a) reported that the Ca/Al ratio between paved road dust and soil dust were differed in Fushun city, North China, which indicates that paved road dust may be influenced heavily by construction materials such as cement. The Ca/Al ratio in materials from the Earth's UCC was significantly lower than that in soil dust in desert regions and urban fugitive dust. Therefore, when the EF method uses the UCC as the reference for evaluating elemental origin, anthropogenic emissions will be overestimated.

The ratios of K, Ti, Mn, and Fe versus Al in the four sample types were relatively constant with those of the UCC. A slight difference was detected when comparing elements to Al ratios among previous studies in desert and Gobi regions in northwestern China. As a result, our study demonstrates that these crustal elements retain the elemental signatures of Asian dust after long–range transport even in polluted areas (Cao et al., 2008). However, heavy metals such as Zn, As, and Pb showed some difference in comparison with dust trace elements. As shown in Table 3, Zn, As, and Pb to Al ratios in construction and cement samples were higher than those in soil samples. In addition, the Zn/Al and Pb/Al ratios in this study were 1.5 to 5 times those in desert soil, Gobi soil, and loess soil samples, indicating that heavy metals such as Zn and Pb can be considered as markers for urban fugitive dust. Previous studies have reported that heavy metals could also be used as marker species in comparison with dust trace elements (Wong et al., 2006; Kong et al., 2011b). In addition, the ratios of V/Al, Cr/Al, and Ni/Al showed no obvious difference in typical soil samples, such as those from Chinese desert regions and Gobi soil, which indicates that these elements have a lesser influence on the anthropogenic sources.

Results on various sizes of fraction samples are shown in Table 2. Because the corresponding dataset was unavailable, these comparisons do not consider differences resulting from the size segregation effect. This is a defect of the present study and will be addressed in future work.

3.2. Origins of elements

The correlation matrix of all elements in all samples is listed in Table 3. Strong correlations ($r=0.841–0.928$, $p<0.0001$) were observed among Al, Si, K, and Ti at all sites, which implies that they had the same sources and can be considered as typical dust trace elements. The correlation coefficients between Ca and Al, Si, and K were from -0.909 to -0.987 ($p<0.0001$). Such strong negative correlations illustrate that the emission sources of Ca and typical dust trace elements should be different and that the abundance of Ca should be linked with an anthropogenic origin. In fact, Ca is the major component in cement samples. Therefore, this negative correlation is likely due to the presence of the cement samples. It is evident that Fe had a weak correlation ($r<0.51$, $p<0.01$) with typical dust trace elements, which indicates that an emission source other than crustal material existed. Previous studies have reported that Fe is a trace element of industry profiles (Yatkin and Bayram, 2008).

The correlation types of heavy metals differ from those of typical dust trace elements. Mn was observed to have positive correlations with crustal elements (Al, Si, K, and Ti), which indicates that Mn has mainly a crustal origin. On the contrary, Zn, As, Pb, and S had negative correlations with dust trace elements, implying different emission sources. As previously mentioned, the ratios of these elements to Al were higher than those in the desert and Gobi soil samples, and the abundance of these elements in fugitive dust implies an influence of additional emissions.

Table 1. Concentrations for the chemical species in urban fugitive dusts over Xi'an

Analyze	Building Construction Dust Mass (µg/g)		Paved Road Dust Mass (µg/g)		Cement Dust Mass (µg/g)		Fresh Soil Dust Mass (µg/g)	
	Mean	Standard Deviation	Mean	Standard Deviation	Mean	Standard Deviation	Mean	Standard Deviation
Al	54 578.09	4 299.83	55 343.45	5 360.94	44 446.70	1 456.70	58 108.30	1 916.71
Si	220 357.59	23 475.65	218 593.92	23 640.42	152 052.52	10 802.58	249 148.22	1 386.43
Na	14 914.58	2 842.37	12 753.80	2 884.56	10 954.60	2 492.84	15 664.50	2 469.03
Mg	15 832.78	1 260.84	16 764.02	1 932.87	12 899.30	890.68	14 502.44	1 052.62
K	15 966.17	2 035.20	15 824.80	2 413.03	9 682.89	1 057.42	18 334.97	2 114.84
Ca	92 951.72	26 240.29	96 721.67	24 945.59	172 804.80	21 369.07	64 426.25	3 987.89
Fe	31 698.97	2 386.44	30 306.49	2 263.38	24 475.67	7 752.67	28 811.41	211.44
S	2 498.28	1 154.69	2 481.34	1 106.84	4 874.47	421.49	1 312.83	793.28
Ti	3 246.59	344.59	3 255.55	266.86	2 375.53	289.81	3 368.41	238.13
V	74.89	4.99	78.36	4.46	73.35	15.95	74.28	3.19
Cr	82.31	8.04	79.66	14.75	65.24	1.66	70.84	3.50
Mn	581.08	46.64	586.66	39.39	504.98	75.76	571.98	2.96
Ni	29.33	2.60	29.87	2.85	23.12	3.71	25.22	2.70
Cu	45.36	8.88	57.94	30.90	39.26	6.38	30.65	2.62
Zn	241.99	112.82	198.63	92.82	161.91	33.87	137.99	30.79
As	16.19	3.84	14.13	1.75	26.57	5.79	9.60	1.01
Pb	92.17	32.70	66.91	24.69	164.36	28.61	43.71	3.78
Cl	2 597.02	3 515.15	871.25	1 297.16	0.00	0.00	2 020.64	2 660.22
Na^+	757.05	740.98	299.50	187.65	848.35	296.07	332.20	76.51
K^+	913.07	465.06	501.18	236.67	1 455.10	182.57	536.70	273.37
Mg^+	272.27	102.84	334.95	58.99	145.80	19.66	302.95	79.13
Ca^{2+}	12 312.04	4 983.90	8 629.40	854.07	39 322.65	21 102.82	8 309.70	558.76
F^-	97.85	33.59	104.50	21.53	130.85	49.00	78.45	10.68
Cl^-	641.79	567.48	462.53	283.96	371.20	121.20	619.55	535.77
NO_2^-	125.16	41.67	124.78	29.16	142.55	49.85	106.95	1.63
NO_3^-	204.47	94.65	196.83	108.98	142.30	42.71	164.85	172.18
SO_4^{2-}	4 511.32	4 058.49	6 064.70	5 657.91	5 445.40	3 511.78	2 404.70	1 703.99

Table 2. Comparison of elemental ratios of urban dusts observed in Xi'an and other regions

Site	Sample Type	Size	Type	Si/Al	K/Al	Ca/Al	Ti/Al	Mn/Al	Fe/Al	Zn/Al (x10³)	As/Al (x10³)	Pb/Al (x10³)	Study
Xi'an, CLP, China	Clayey Loess	TSP	Soil dust	2.97	0.32	0.95	0.05	0.01	0.57	1.63	0.27	0.69	Cao et al. (2008)
Desert soil	Source	<100 μm	Soil	7.68	0.34	0.94	0.06	0.01	0.54	0.68	0.15	0.26	Ta et al. (2003)
Gobi soil	Source	<100 μm	Soil dust	7.85	0.39	1.17	0.04	0.01	0.35	0.55	0.15	0.39	Ta et al. (2003)
Gosan, South Korea	Ambient	TSP	Soil dust	1.44	0.28	0.56	0.05	NA [a]	0.48	NA [a]	NA [a]	NA [a]	Arimoto et al. (2006)
Earth's Upper Continental Crust	Source		Soil	3.83	0.35	0.37	0.04	0.01	0.44	NA [a]	NA [a]	0.00	Taylor and Mclennan (1995)
Mexico City		PM$_{2.5}$	Cement dust	7.92	0.52	65.00	0.00	0.01	0.73	0.00	12.50	0.00	Vega et al. (2001)
			Paved road dust	3.26	0.19	0.96	0.06	0.01	0.75	16.42	0.00	7.17	
		PM$_{10}$	Cement dust	6.11	0.33	35.22	0.02	0.01	0.59	1.11	6.67	0.00	
			Paved road dust	3.17	0.15	0.73	0.05	0.01	0.49	9.72	0.00	4.93	
Hong Kong, China		PM$_{2.5}$	Cement dust	3.93	1.10	29.47	0.09	0.03	1.35	36.29	1.38	11.47	Ho et al. (2003a)
			Paved road dust	2.56	0.40	1.93	0.05	0.03	1.65	147.72	0.37	30.15	
		PM$_{10}$	Cement dust	3.62	0.39	17.28	0.05	0.01	0.79	16.18	0.66	4.92	
			Paved road dust	2.59	0.29	1.19	0.03	0.01	0.68	69.26	0.05	14.27	
California, USA	Fugitive dust	PM$_{10}$	Paved road dust	2.93	0.35	0.45	0.05	0.01	0.56	9.65	0.16	1.09	Chow et al. (2003)
			Construction dust	3.10	0.27	0.42	0.04	0.01	0.37	2.30	0.06	0.68	
Fushun, China		PM$_{10}$	Paved road dust	1.79	0.08	2.89	0.06	0.01	0.14	8.89	0.22	0.76	Kong et al. (2011a)
			Soil dust	1.26	0.06	0.61	0.04	0.01	0.17	14.81	0.24	3.48	
Xi'an, China			Soil dust	4.29	0.32	1.11	0.06	0.01	0.50	2.37	0.17	0.75	This study
			Cement	3.42	0.22	3.90	0.05	0.01	0.55	3.64	0.60	3.70	
		<100 μm	Construction dust	4.02	0.29	1.69	0.06	0.01	0.61	4.43	0.30	1.69	
			Paved road dust	4.05	0.29	1.48	0.06	0.01	0.54	3.59	0.26	1.21	

[a] *Not Available*

Table 3. Summary of correlation coefficients of selected species in urban fugitive dust over Xi'an

	Na	Mg	Al	Si	K	Ca	Fe	S	P	Ti	V	Cr	Mn	Ni	Cu	Zn	As	Pb	Ba
Na	1.000																		
Mg	-0.096	1.000																	
Al	0.219	0.310	1.000																
Si	0.422[a]	0.168	0.909[a]	1.000															
K	0.440[a]	0.316	0.929[a]	0.928[a]	1.000														
Ca	-0.468[a]	-0.197	-0.909[a]	-0.987[a]	-0.937[a]	1.000													
Fe	0.511[a]	0.154	0.503[a]	0.482[a]	0.466[a]	-0.569[a]	1.000												
S	-0.057	-0.008	-0.566[a]	-0.642[a]	-0.542[a]	0.606[a]	-0.211	1.000											
P	0.239	0.454[a]	0.342	0.312	0.390	-0.357	0.325	-0.021	1.000										
Ti	0.330	0.160	0.909[a]	0.912[a]	0.841[a]	-0.924[a]	0.623[a]	-0.614[a]	0.307	1.000									
V	-0.150	0.253	0.428[a]	0.277	0.379	-0.287	0.273	-0.289	-0.013	0.305	1.000								
Cr	0.489[a]	0.287	0.136	0.234	0.165	-0.293	0.633[a]	0.172	0.324	0.262	-0.180	1.000							
Mn	0.458[a]	0.162	0.689[a]	0.647[a]	0.699[a]	-0.681[a]	0.684[a]	-0.436[a]	0.095	0.761[a]	0.558[a]	0.256	1.000						
Ni	0.162	0.298	0.572[a]	0.561[a]	0.472[a]	-0.591[a]	0.615[a]	-0.373	0.349	0.615[a]	0.311	0.449[a]	0.460[a]	1.000					
Cu	0.248	0.308	-0.155	-0.122	-0.129	0.062	0.245	0.242	0.133	-0.115	-0.149	0.576[a]	-0.077	0.343	1.000				
Zn	0.008	-0.007	-0.509[a]	-0.406[a]	-0.468[a]	0.359	0.187	0.219	0.068	-0.371	-0.388	0.269	-0.394	-0.059	0.331	1.000			
As	-0.227	-0.263	-0.525[a]	-0.675[a]	-0.648[a]	0.649[a]	-0.060	0.446[a]	-0.177	-0.520[a]	-0.066	-0.012	-0.333	-0.141	0.186	0.094	1.000		
Pb	-0.158	-0.306	-0.643[a]	-0.728[a]	-0.739[a]	0.704[a]	-0.068	0.478[a]	-0.143	-0.600[a]	-0.296	0.054	-0.474[a]	-0.169	0.278	0.320	0.941[a]	1.000	
Ba	0.113	0.000	-0.039	-0.069	-0.131	0.022	0.205	0.027	0.078	-0.065	-0.275	0.397	-0.110	0.086	0.421	0.211	0.155	0.250	1.000

[a] $p < 0.01$

Enrichment factors (EFs) were calculated in these samples to further investigate whether the elemental origin was a natural source or of anthropogenic emission. Figure 2 plotted the EFs of abundant elements including Na, Mg, Al, Si, K, Ca, Fe, Ti, V, Cr, Mn, Co, Ni, Cu, Zn, As, Ba, and Pb. EF<5 is usually considered as crustal origin. Unlike the aerosol samples, the EFs of fugitive dust samples were generally low. The enrichment factor values indicate that continental crust was the dominant source for elements such as Na, Mg, Al, Si, K, Ti, V, Mn, Co, Ni, and Ba in fugitive dust samples in Xi'an. With the exception of Ca, As, and Pb, no obvious difference was noted for elemental EF values among the four sample types. Compared with that in the crustal elements (Si, Al, K, Ti, and Fe), the EFs for Ca in cement samples, As in all samples, and Pb in construction and cement samples were 2–10 times higher than those of other elements. A similar trend was observed between Pb and Ca, which indicates that both were influenced by the same sources in the construction area. The abundance of Pb and As in the samples, potentially toxic trace elements, indicates that the vehicle emissions and the combustion of coal and bio–fuel also affect soil in the entire city. Previous studies have reported that As and Pb were detected in Chinese coal (Tian et al., 2011; Xu et al., 2012), although Pb was discontinued as a gasoline additive in 2000 (Xu et al., 2012). Zn normally originates from the metal smelting industry and vehicle tire wear (Sammut et al., 2006). High levels of toxic elements in fugitive dust in comparison with desert and Gobi soil implies a severe health risk if disbursed into the air. Ca, As, and Pb were enriched in cement mainly due to the ore calcination processes in cement production. Kong et al. (2011a) also deter-mined that these three elements were abundant in cement samples.

3.3. Water–soluble ion levels

The average concentrations and standards deviations of measured water–soluble ions in four types of samples are listed in Table 1. Generally, total water–soluble ions only occupied 2.0%, 1.7%, 4.8%, and 1.3% in construction dust, paved road dust, cement, and soil dust, respectively, which indicates that most of the material in fugitive dust is insoluble. Ca^{2+} was the most abundant ion among all samples, particularly in construction and cements samples, followed by SO_4^{2-}. Ca^{2+} and SO_4^{2-} accounted for 60% and 23% in total ion mass, respectively. The other ion distributions in construction and cement samples were followed the sequence of $K^+>Na^+>Cl^->Mg^{2+}>NO_3^-$. Cl^- prevailed against K^+ in soil dust samples and Cl^- and Mg^{2+} prevailed against Na^+ in paved road dust samples. Thus, high Ca and Ca^{2+} should be the markers of construction dust and cement samples. SO_4^{2-} levels varied from 2.4‰ in soil dust to 6.0‰ in paved road dust among the four sample types, which reflects slight pollution in paved road dust, cement, and construction dust samples. NO_3^- levels in all samples were significantly lower than sulfate. Poor correlations were observed among sulfate and nitrate with dust trace elements and cations, which reveals that these two species may have anthropogenic sources. However, considering the lowest levels in surface fugitive dust samples in comparison with high levels in urban aerosol particles (Shen et al., 2009a), the anthropogenic influence on sulfate and nitrate is negligible.

K^+/K and Ca^{2+}/Ca ratios were calculated to detect the phase states of K and Ca. In general, K^+/K and Ca^{2+}/Ca ratios were both slightly high in cement and construction samples but were lower in paved road dust and soil dust samples. K^+/K ratios ranged from 0.03 in soil dust to 0.15 in cement samples, and Ca^{2+}/Ca ranged from 0.09 in paved road dust to 0.23 in cement samples. However, that K^+/K and Ca^{2+}/Ca ratios both had low values in urban dust samples in comparison with urban aerosol particles. Prior research demonstrated that soil dust from desert and Gobi regions exhibited high Ca^{2+} and Ca concentrations and that the Ca^{2+}/Ca ratio reached 0.74 during a dust storm event (Shen et al., 2007). Therefore, urban fugitive dust in Xi'an is characterized by high insoluble Ca in

comparison with Gobi and desert soil dust. K^+ is considered as the biomass burning marker and is popularly applied in aerosol source identification (Andreae, 1983; Shen et al., 2009a). The K^+/K ratio was only 0.1 in dust storm samples but increased to 0.55 during pollution events (Shen et al., 2007). The present study reveals that the potential contribution of urban fugitive dusts to water–soluble K is insignificant and further demonstrates that K^+ can be considered as a marker for biomass burning emission.

3.4. Ion balance and carbonate estimation

Ion balance calculations can be used as an approach for studying the acid–base balances of ions measured in aerosol particle samples (Shen et al., 2009a). Here, this method was used to evaluate the cation and anion balances of surface fugitive dust samples. The alkalinity was determined on the basis of the following equations:

$$C\left(cation\ microequivalents\ \frac{1}{m^3}\right)$$
$$= \frac{Na^+}{23} + \frac{NH_4^+}{18} + \frac{K^+}{39} + \frac{Mg^{2+}}{12} + \frac{Ca^{2+}}{20} \quad (2)$$
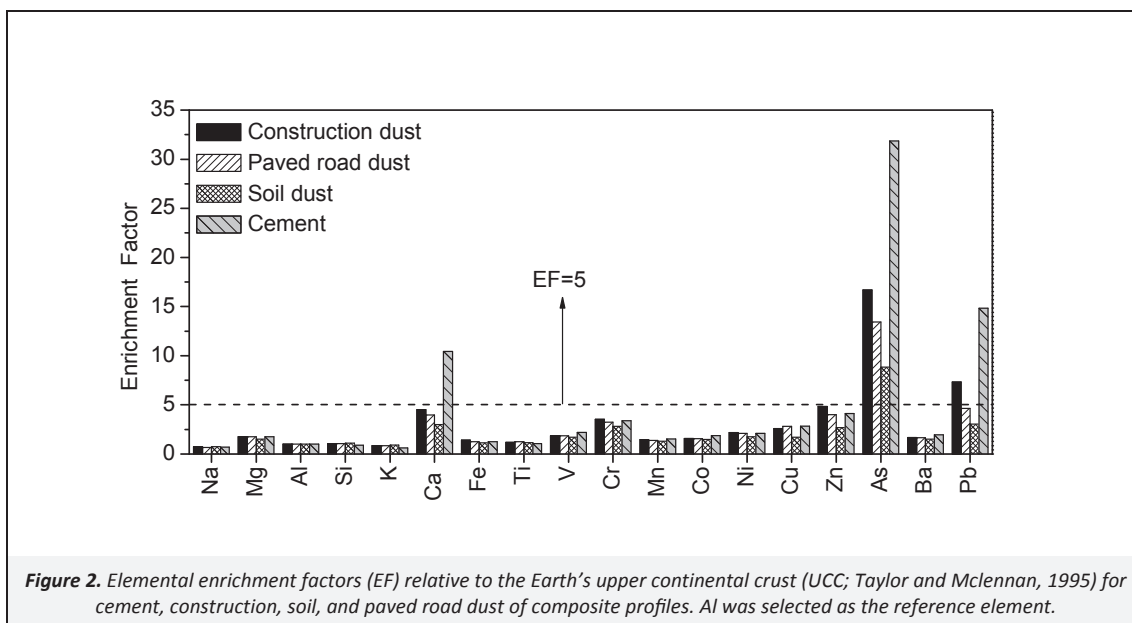
$$C\left(anion\ microequivalents\ \frac{1}{m^3}\right)$$
$$= \frac{F^-}{19} + \frac{Cl^-}{35.5} + \frac{NO_3^-}{62} + \frac{SO_4^{2-}}{48} \quad (3)$$

Ion balance calculations showed that the A/C ratios of most samples were much lower than the unity (averaged at 0.19), which implies that the urban fugitive dusts were more alkaline and that the apparent deficit of anions is likely due to the existence of carbonate (CO_3^{2-}), according to the occurrence of carbonate in soil dust (Cao et al., 2005; Shen et al., 2007). Although other anions such as CH_3COO^-, $HCOO^-$, $C_2O_4^{2-}$, and PO_4^{3-}, were not investigated in this study, we do not consider them related to the anion deficit due to their low masses in the samples (Wang et al., 2005). Previous studies have in fact documented the occurrence of carbonate in Asian dust (Xu et al., 2004; Cao et al., 2005; Shen et al., 2009b). In addition, Chinese loess is characteristically richer in calcite (approximately 100%) than dolomite (Wen, 1989). Previous literature reported a simple method that uses the ion balance difference for direct calculation of the mass concentration of CO_3^{2-} in aerosol samples and verifies that the measured carbonate concentrations are consistent with the estimation results (Clarke and Karani, 1992; Shen et al., 2007; Ho et al., 2011; Shen et al., 2011). Following this method, good correlation was observed between the estimated levels of CO_3^{2-} and Ca^{2+} with a high correlation coefficient value of 0.97. Moreover, the slope of the regression line (0.65) shows a best fit to the mass ratio of Ca^{2+}/CO_3^{2-} (0.67), further demonstrating the accuracy of the carbonate estimation method. However, when stratifying by sample type, the highest levels CO_3^{2-} were detected in cement samples. This result occurred mainly because calcite is the one of the major components in cement production.

3.5. Comparability of fugitive dust chemical profiles

The coefficient of divergence (CD), a self–normalizing parame-ter, was adopted to compare the similarities between the chemical profiles of fugitive dust. The CD is calculated as follows:

$$CD_{jk} = \sqrt{\frac{1}{p}\sum_{i=1}^{p}\left(\frac{x_{ij}-x_{ik}}{x_{ij}+x_{ik}}\right)^2} \quad (4)$$

Figure 2. Elemental enrichment factors (EF) relative to the Earth's upper continental crust (UCC; Taylor and Mclennan, 1995) for cement, construction, soil, and paved road dust of composite profiles. Al was selected as the reference element.

where, x_{ij} represents the average concentration for a chemical component i at site j, j and k represent two sampling sites, and p is the number of chemical components (Wongphatarakul et al., 1998). A CD approaching zero supports the null hypothesis, that is, that the two types of samples were similar for the measured chemical species. If the chemical composition at the two sampling sites were very different, the CD would approach unity. The CD values of fugitive dust in Xi'an were calculated in Table 4.

Table 4. Coefficient of divergence (CD) values for similarity comparison among four types of fugitive dust in Xi'an

CD	Building Construction Dust	Paved Road Dust	Fresh Soil Dust	Cement Dust
Building construction dust	0	0.12	0.12	0.19
Paved road dust		0	0.11	0.24
Fresh soil dust			0	0.25
Cement dust				0

The calculated CD values were generally low, indicated that the chemical composition were quite similar in special sample sites over Xi'an. It was noted that the CD values were the highest between cement dust and other type fugitive dusts, revealed that cement dust was somewhat dissimilar with others. In contrast, the chemical profiles among building construction dust, paved road dust, and fresh soil dust were nearly similar.

4. Conclusion

The elemental composition of urban fugitive dust was determined and compared with that reported in previous studies. The results showed that the properties of dust trace elements such as Al, Si, Mn, and Ti are similar to those in loess and soil dust from the desert and Gobi areas in northern China. In contrast, Ca, As, and Pb, particularly in the construction and cement samples, were shown to be influenced by anthropogenic sources. Most of the materials in urban fugitive dust samples were in insoluble phases, and the total water soluble components were lower than 5% in the collected samples. Ca^{2+} was the most abundant ion in all samples and formed $CaCO_3$ in the urban fugitive dust samples. SO_4^{2-} and NO_3^- levels were negligible when compared with urban aerosol samples. Low Ca^{2+}/Ca and K^+/K ratios were detected, which supplied other markers for distinguishing fugitive dust with combustion emissions.

The present study focused on the chemical profiles of bulk fugitive soil dust. Further study is needed to evaluate the chemical composition of fugitive dust samples in different size fractions by using the re–suspension method, which is important for source apportionment.

References

Abdul–Wahab, S.A., 2006. Impact of fugitive dust emissions from cement plants on nearby communities. *Ecological Modelling* 195, 338–348.

Acosta, J.A., Faz, A., Kalbitz, K., Jansen, B., Martinez–Martinez, S., 2011. Heavy metal concentrations in particle size fractions from street dust of Murcia (Spain) as the basis for risk assessment. *Journal of Environmental Monitoring* 13, 3087–3096.

Alfaro, S.C., Gomes, L., Rajot, J.L., Lafon, S., Gaudichet, A., Chatenet, B., Maille, M., Cautenet, G., Lasserre, F., Cachier, H., Zhang, X.Y., 2003. Chemical and optical characterization of aerosols measured in spring 2002 at the ACE–Asia supersite, Zhenbeitai, China. *Journal of Geophysical Research–Atmospheres* 108, art. no. 8641.

Amato, F., Pandolfi, M., Viana, M., Querol, X., Alastuey, A., Moreno, T., 2009. Spatial and chemical patterns of PM_{10} in road dust deposited in urban environment. *Atmospheric Environment* 43, 1650–1659.

Andreae, M.O., 1983. Soot carbon and excess fine potassium – long–range transport of combustion–derived aerosols. *Science* 220, 1148–1151.

Arimoto, R., Kim, Y.J., Kim, Y.P., Quinn, P.K., Bates, T.S., Anderson, T.L., Gong, S., Uno, I., Chin, M., Huebert, B.J., Clarke, A.D., Shinozuka, Y., Weber, R.J., Anderson, J.R., Guazzotti, S.A., Sullivan, R.C., Sodeman, D.A., Prather, K.A., Sokolik, I.N., 2006. Characterization of Asian Dust during ACE–Asia. *Global and Planetary Change* 52, 23–56.

Arimoto, R., Zhang, X.Y., Huebert, B.J., Kang, C.H., Savoie, D.L., Prospero, J.M., Sage, S.K., Schloesslin, C.A., Khaing, H.M., Oh, S.N., 2004. Chemical composition of atmospheric aerosols from Zhenbeitai, China, and Gosan, South Korea, during ACE–Asia. *Journal of Geophysical Research–Atmospheres* 109, art. no. D19S04.

Ashbaugh, L.L., Carvacho, O.F., Brown, M.S., Chow, J.C., Watson, J.G., Magliano, K.C., 2003. Soil sample collection and analysis for the Fugitive Dust Characterization Study. *Atmospheric Environment* 37, 1163–1173.

Bhaskar, V.S., Sharma, M., 2008. Assessment of fugitive road dust emissions in Kanpur, India: A note. *Transportation Research Part D–Transport and Environment* 13, 400–403.

Cao, J.J., Shen, Z.X., Chow, J.C., Watson, J.G., Lee, S.C., Tie, X.X., Ho, K.F., Wang, G.H., Han, Y.M., 2012a. Winter and summer $PM_{2.5}$ chemical compositions in fourteen Chinese cities. *Journal of the Air & Waste Management Association* 62, 1214–1226.

Cao, J.J., Wang, Q.Y., Chow, J.C., Watson, J.G., Tie, X.X., Shen, Z.X., Wang, P., An, Z.S., 2012b. Impacts of aerosol compositions on visibility impairment in Xi'an, China. *Atmospheric Environment* 59, 559–566.

Cao, J.J., Chow, J.C., Watson, J.G., Wu, F., Han, Y.M., Jin, Z.D., Shen, Z.X., An, Z.S., 2008. Size–differentiated source profiles for fugitive dust in the Chinese Loess Plateau. *Atmospheric Environment* 42, 2261–2275.

Cao, J.J., Lee, S.C., Zhang, X.Y., Chow, J.C., An, Z.S., Ho, K.F., Watson, J.G., Fung, K., Wang, Y.Q., Shen, Z.X., 2005. Characterization of airborne carbonate over a site near Asian dust source regions during spring 2002 and its climatic and environmental significance. *Journal of Geophysical Research: Atmospheres* 110, art. no. D03203.

Cesari, D., Contini, D., Genga, A., Siciliano, M., Elefante, C., Baglivi, F., Daniele, L., 2012. Analysis of raw soils and their re–suspended PM_{10} fractions: Characterisation of source profiles and enrichment factors. *Applied Geochemistry* 27, 1238–1246.

Cheng, Y., Zou, S.C., Lee, S.C., Chow, J.C., Ho, K.F., Watson, J.G., Han, Y.M., Zhang, R.J., Zhang, F., Yau, P.S., Huang, Y., Bai, Y., Wu, W.J., 2011. Characteristics and source apportionment of PM_1 emissions at a roadside station. *Journal of Hazardous Materials* 195, 82–91.

Chow, J.C., Watson, J.G., Ashbaugh, L.L., Magliano, K.L., 2003. Similarities and differences in PM_{10} chemical source profiles for geological dust from the San Joaquin Valley, California. *Atmospheric Environment* 37, 1317–1340.

Chow, J.C., Chung Shing, L., Cassmassi, J., Watson, J.G., Lu, Z., Pritchett, L.C., 1992a. A neighborhood–scale study of PM_{10} source contributions in Rubidoux, California. *Atmospheric Environment. Part A. General Topics* 26, 693–706.

Chow, J.C., Watson, J.G., Lowenthal, D.H., Solomon, P.A., Magliano, K.L., Ziman, S.D., Willard Richards, L., 1992b. PM_{10} source apportionment in California's San Joaquin Valley. *Atmospheric Environment. Part A. General Topics* 26, 3335–3354.

Clarke, A.G., Karani, G.N., 1992. Characterization of the carbonate content of atmospheric aerosols. *Journal of Atmospheric Chemistry* 14, 119–128.

Han, L.H., Zhuang, G.S., Cheng, S.Y., Wang, Y., Li, J., 2007. Characteristics of re–suspended road dust and its impact on the atmospheric environment in Beijing. *Atmospheric Environment* 41, 7485–7499.

Ho, K.F., Zhang, R.J., Lee, S.C., Ho, S.S.H., Liu, S.X., Fung, K., Cao, J.J., Shen, Z.X., Xu, H.M., 2011. Characteristics of carbonate carbon in $PM_{2.5}$ in a typical semi–arid area of Northeastern China. *Atmospheric Environment* 45, 1268–1274.

Ho, K.F., Lee, S.C., Chow, J.C., Watson, J.G., 2003a. Characterization of PM_{10} and $PM_{2.5}$ source profiles for fugitive dust in Hong Kong. *Atmospheric Environment* 37, 1023–1032.

Ho, K.F., Lee, S.C., Chan, C.K., Yu, J.C., Chow, J.C., Yao, X.H., 2003b. Characterization of chemical species in $PM_{2.5}$ and PM_{10} aerosols in Hong Kong. *Atmospheric Environment* 37, 31–39.

Kong, S., Ji, Y., Lu, B., Chen, L., Han, B., Li, Z., Bai, Z., 2011a. Characterization of PM_{10} source profiles for fugitive dust in Fushun–a city famous for coal. *Atmospheric Environment* 45, 5351–5365.

Kong, S., Lu, B., Ji, Y., Zhao, X., Chen, L., Li, Z., Han, B., Bai, Z., 2011b. Levels, risk assessment and sources of PM_{10} fraction heavy metals in four types dust from a coal–based city. *Microchemical Journal* 98, 280–290.

Pietrodangelo, A., Salzano, R., Rantica, E., Perrino, C., 2013. Characterisation of the local topsoil contribution to airborne particulate matter in the area of Rome (Italy). Source profiles. *Atmospheric Environment* 69, 1–14.

Rhodes, J.R., Pradzynski, A.H., Hunter, C.B., Payne, J.S., Lindgren, J.L., 1972. Energy dispersive x–ray fluorescence analysis of air particulates in Texas. *Environmental Science & Technology* 6, 922–927.

Sammut, M.L., Noack, Y., Rose, J., 2006. Zinc speciation in steel plant atmospheric emissions: A multi–technical approach. *Journal of Geochemical Exploration* 88, 239–242.

Shen, Z.X., Zhang, L.M., Cao, J.J., Tian, J., Liu, L., Wang, G.H., Zhao, Z.Z., Wang, X., Zhang, R.J., Liu, S.X., 2012. Chemical composition, sources, and deposition fluxes of water–soluble inorganic ions obtained from precipitation chemistry measurements collected at an urban site in northwest China. *Journal of Environmental Monitoring* 14, 3000–3008.

Shen, Z.X., Wang, X., Zhang, R.J., Ho, K.F., Cao, J.J., Zhang, M.G., 2011. Chemical composition of water–soluble ions and carbonate estimation in spring aerosol at a semi–arid site of Tongyu, China. *Aerosol and Air Quality Research* 11, 360–368.

Shen, Z., Cao, J., Arimoto, R., Han, Z., Zhang, R., Han, Y., Liu, S., Okuda, T., Nakao, S., Tanaka, S., 2009a. Ionic composition of TSP and $PM_{2.5}$ during dust storms and air pollution episodes at Xi'an, China. *Atmospheric Environment* 43, 2911–2918.

Shen, Z.X., Caquineau, S., Cao, J.J., Zhang, X.Y., Han, Y.M., Gaudichet, A., Gomes, L., 2009b. Mineralogical characteristics of soil dust from source regions in northern China. *Particuology* 7, 507–512.

Shen, Z.X., Cao, J.J., Arimoto, R., Zhang, R.J., Jie, D.M., Liu, S.X., Zhu, C.S., 2007. Chemical composition and source characterization of spring aerosol over Horqin sand land in northeastern China. *Journal of Geophysical Research–Atmospheres* 112, art. no. D14315.

Ta, W.Q., Xiao, Z., Qu, J.J., Yang, G.S., Wang, T., 2003. Characteristics of dust particles from the desert/Gobi area of northwestern China during dust–storm periods. *Environmental Geology* 43, 667–679.

Taylor, S.R., Mclennan, S.M., 1995. The geochemical evolution of the continental–crust. *Reviews of Geophysics* 33, 241–265.

Tian, H.Z., Wang, Y., Xue, Z.G., Qu, Y.P., Chai, F.H., Hao, J.M., 2011. Atmospheric emissions estimation of Hg, As, and Se from coal–fired power plants in China, 2007. *Science of the Total Environment* 409, 3078–3081.

Vega, E., Mugica, V., Reyes, E., Sanchez, G., Chow, J.C., Watson, J.G., 2001. Chemical composition of fugitive dust emitters in Mexico City. *Atmospheric Environment* 35, 4033–4039.

Wang, Y., Zhuang, G., Sun, Y., An, Z., 2005. Water–soluble part of the aerosol in the dust storm season—evidence of the mixing between mineral and pollution aerosols. *Atmospheric Environment* 39, 7020–7029.

Wen, Q.Z., 1989. *Chinese Loess Geochemistry*, Sci. Press, Beijing, pp. 115–158 (in Chinese).

Wong, C.S.C., Li, X.D., Thornton, I., 2006. Urban environmental geochemistry of trace metals. *Environmental Pollution* 142, 1–16.

Wongphatarakul, V., Friedlander, S.K., Pinto, J.P., 1998. A comparative study of $PM_{2.5}$ ambient aerosol chemical databases. *Environmental Science & Technology* 32, 3926–3934.

Wu, F., Chow, J.C., An, Z.S., Watson, J.G., Cao, J.J., 2011. Size–differentiated chemical characteristics of Asian paleo dust: Records from aeolian deposition on Chinese Loess Plateau. *Journal of the Air & Waste Management Association* 61, 180–189.

Xu, H.M., Cao, J.J., Ho, K.F., Ding, H., Han, Y.M., Wang, G.H., Chow, J.C., Watson, J.G., Khol, S.D., Qiang, J., Li, W.T., 2012. Lead concentrations in fine particulate matter after the phasing out of leaded gasoline in Xi'an, China. *Atmospheric Environment* 46, 217–224.

Xu, J., Bergin, M.H., Greenwald, R., Schauer, J.J., Shafer, M.M., Jaffrezo, J.L., Aymoz, G., 2004. Aerosol chemical, physical, and radiative characteristics near a desert source region of northwest China during ACE–Asia. *Journal of Geophysical Research: Atmospheres* 109, art. no. D19S03.

Yang, F., Tan, J., Zhao, Q., Du, Z., He, K., Ma, Y., Duan, F., Chen, G., Zhao, Q., 2011. Characteristics of PM$_{2.5}$ speciation in representative megacities and across China. *Atmospheric Chemistry and Physics* 11, 5207–5219.

Yatkin, S., Bayram, A., 2008. Determination of major natural and anthropogenic source profiles for particulate matter and trace elements in Izmir, Turkey. *Chemosphere* 71, 685–696.

Zhang, R.J., Arimoto, R., An, J.L., Yabuki, S., Sun, J.H., 2005. Ground observations of a strong dust storm in Beijing in March 2002. *Journal of Geophysical Research–Atmospheres* 110, art. no. 18S06.

Zhang, X.Y., Gong, S.L., Shen, Z.X., Mei, F.M., Xi, X.X., Liu, L.C., Zhou, Z.J., Wang, D., Wang, Y.Q., Cheng, Y., 2003. Characterization of soil dust aerosol in China and its transport and distribution during 2001 ACE–Asia: 1. Network observations. *Journal of Geophysical Research: Atmospheres* 108, art. no. 4261.

Zhang, X.Y., Cao, J.J., Li, L.M., Arimoto, R., Cheng, Y., Huebert, B., Wang, D., 2002. Characterization of atmospheric aerosol over XiAn in the south margin of the Loess Plateau, China. *Atmospheric Environment* 36, 4189–4199.

Zhao, Q., He, K.B., Rahn, K.A., Ma, Y.L., Yang, F.M., Duan, F.K., 2010. Using SI depletion in aerosol to identify the sources of crustal dust in two Chinese megacities. *Atmospheric Environment* 44, 2615–2624.